Int. J. Multiphase Flow Vol. 19, No. 5, pp. 817–828, 1993
Printed in Great Britain.

0301-9322/93 $6.00 + 0.00

VOID DISTRIBUTION IN SLUG FLOW†

P. ANDREUSSI,[1] K. H. BENDIKSEN[2] and O. J. NYDAL[2]

[1]Department of Chemical Sciences and Technologies, University of Udine, Via del Cotonificio 108, 33100 Udine, Italy

[2]Institute for Energy Technology, 2007 Kjeller, Norway

(Received 31 July 1991; in revised form 1 June 1993)

Abstract—Air–water slug flow at atmospheric conditions in horizontal pipes of 31 and 53 mm i.d. has been characterized experimentally with local (optical) and cross-sectional (conductance) probes. The objective of the work is to improve the description of slug flow and the closure relations required in mean kinematic slug flow models. Local measurements include the radial void fraction distribution in the slugs, the size of the dispersed bubbles in the slug and the aeration of the liquid layer under the slug bubble. From cross-sectional holdup measurements, slug lengths and frequencies are determined, as well as the length of the highly aerated mixing zone in the front of the slugs. Measured values of film holdup at the tail of the slug bubbles and of slug frequency are compared with a physical model of slug flow derived from the work of Dukler & Hubbard.

Key Words: slug flow, void fraction, void distribution, slug frequency

1. INTRODUCTION

Slug flow in near-horizontal pipes can be described as a stratified flow with the intermittent appearance of aerated liquid slugs traveling at high velocity. In modeling this flow pattern an averaged 1-D model is usually selected. This approach is based on the assumption that slug flow can be described as a sequence of slug units traveling at a constant translational velocity (Dukler & Hubbard 1975). The unit is formed by a liquid slug of given length and uniform void followed by a long, turbulent gas bubble flowing above a stratified liquid layer. A complete separation of the phases is assumed in the slug bubble: there are no entrained drops in the gas phase, nor any gas bubbles in the liquid film. The liquid slug region is treated as fully developed bubbly flow and it is usually assumed that the slip between gas and liquid in the slug body is negligible.

The objective of the present investigation is to improve the physical description of slug flow and the experimental basis required in the development of flow models. To this purpose, the void distribution in the slug unit has been analyzed by local (optical) and cross-sectional (impedance) probes.

The experimental observations presented in this paper and the extensive statistical investigation of the main slug parameters completed by Nydal *et al.* (1992) allow a fairly precise description of slug flow. In particular, Nydal *et al.* (1992) presented the statistical distributions of the slug velocity, mean void in the slugs and slug length. In this work, data relative to the 3-D void distribution in a slug are presented along with measurements of slug frequency and more accurate data relative to the total length of the slugs and the length of the more aerated, mixing zone at the front of a slug.

Data relative to the slug frequency and the minimum height of the stratified liquid layer below the slug bubble have been compared with the predictions of a physical model of slug flow derived from the original work of Dukler & Hubbard (1975). Recently, Andreussi *et al.* (1993) have shown that a simplified version of this model gives a very good fit to a large set of data relative to the measurement of the pressure gradient and the mean liquid holdup in slug flow. The present, more accurate description of slug flow should be considered as a first step in the development of a dynamic model capable of predicting (for given input flows, initial conditions and pipe geometry) the evolution of the flow along the pipe and the formation of long slugs. To this end, knowledge

†Presented at the *Int. Conf. on Multiphase Flows*, Tsukuba, Japan, 24–27 September 1991.

of the void distribution in the slug body and of the processes of gas entrainment and disengagement are essential.

2. EXPERIMENTAL SETUP

The test section consists of two horizontal pipes of 31 and 53 mm. The test fluids were water and air at atmospheric conditions. Single-phase flow rates have been measured with calibrated rotameters before the mixing section. All reported superficial gas velocities are at standard conditions (1 bar, 20°C). Further details about the flow loop are reported in Nydal *et al.* (1992).

The instantaneous, cross-section averaged liquid holdup has been measured with the impedance method described in detail and tested by Andreussi *et al.* (1988). The local void fraction has been measured by a fiber optic probe developed by Annunziato (1986). This probe has a sensitive tip 0.7 mm in diameter and, as shown in figure 1, it has been mounted on a micrometric head in order to determine the void distribution profiles in the pipe cross-section. For this purpose, the signal from the probe has been analyzed with a Le Croy 9400 digital oscilloscope. The oscilloscope can operate as a transient recorder activated by a trigger. In these experiments the trigger, which is also shown in figure 1, was made of two quarters of a conducting ring facing each other vertically in a cross section of the pipe immediately before the optical probe. The trigger was operated with the electronics normally employed for conductance probes.

When a slug arrives at, or leaves, the trigger, the transient recorder is activated and the signal from the optical probe is stored. The transient recorder allows the superposition of a large number of slugs, and allows data acquisition to be activated by a positive or negative derivative of the signal arriving from the trigger. In this way it is possible to characterize the void distribution in front or at the back of a slug. In the present experiments, the mean slug velocities have also been measured by two trigger probes, adopting the method described by Nydal *et al.* (1992).

3. FLOW MODEL

Dukler & Hubbard (1975) assumed that slug flow can be represented by a sequence of identical slug units traveling at a constant translational velocity, v_t, that the slip between the gas and liquid in the slug body is negligible and that the liquid film following the slug does not contain dispersed bubbles.

The present observations indicate that the presence of dispersed bubbles in the films is appreciable for high-velocity air–water flow, and is possibly more important for the flow of a low-surface-tension liquid. This phenomenon has a limited direct effect on the mean liquid holdup and on the pressure gradient, but it may be significant in determining the overall void distribution in the slug unit and, in particular, in the slug body. For this reason, the model which is proposed in the following explicitly considers the presence of dispersed bubbles in the liquid film, assuming that they travel at the mean velocity of the liquid and that, due to buoyancy, they are progressively released from the film.

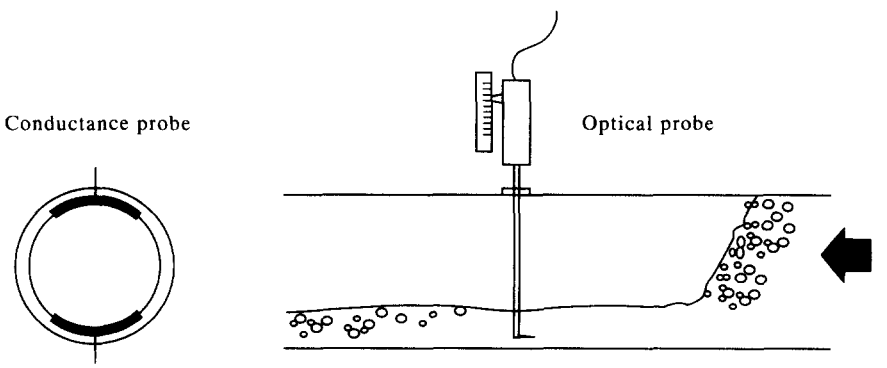

Figure 1. Schematic diagram of a conductance probe and the use of a local optical holdup probe.

The flow model is based on the mass conservation equations for the liquid and gas in a slug unit:

$$j_L = \frac{1}{l_u}\int_0^{l_f} v_f a_f h_f \, dX + h_s v_s \frac{l_s}{l_u} \quad [1]$$

and

$$j_G = \frac{1}{l_u}\int_0^{l_f} [v_f a_f (1-h_f) + v_b(1-a_f)] \, dX + (1-h_s)v_s \frac{l_s}{l_s}, \quad [2]$$

where j is superficial velocity, v is velocity, l is length, h is liquid holdup, subscripts L and G indicate liquid and gas, s the slug body, f the aerated liquid film, u the slug unit and b the gas phase in the stratified flow region, a_f is the fraction of the cross-sectional area occupied by the aerated film and X is the axial coordinate along the slug unit.

The translational velocity of the slug unit is usually expressed as

$$v_t = c_0 v_s + v_0. \quad [3]$$

In [3], v_0 becomes negligible and $c_0 \simeq 1.2$ for large values of the mixture velocity or, as suggested by Bendiksen (1984), when the bubble nose becomes centered.

When the slip between the gas and liquid in the slug body is neglected, the continuity equations relative to an observer traveling at v_t can be written as:

$$(v_t - v_f)a_f h_f = (v_t - v_s)h_s \quad [4]$$

and

$$(v_t - v_b)(1-a_f) + (v_t - v_f)a_f(1-h_f) = (v_t - v_s)(1-h_s). \quad [5]$$

From [1], [2], [4] and [5], it can easily be shown that

$$v_b(1-a_f) + v_f a_f = j_m \quad [6]$$

and

$$v_s = j_m \quad [7]$$

where $j_m = j_L + j_G$ is the mixture velocity.

The mean liquid holdup in the slug unit, h_L, defined as

$$h_L = \frac{h_s l_s + \overline{a_f h_f} l_f}{l_u} \quad [8]$$

where

$$\overline{a_f h_f} = \frac{1}{l_f}\int_0^{l_f} a_f h_f \, dX, \quad [9]$$

can be computed from [1] and [4] as

$$h_L = \frac{j_L + h_s(v_t - v_s)}{v_t}. \quad [10]$$

It is interesting to notice that h_L is entirely independent of the void distribution in the stratified flow region.

The shape and length of the slug tail can be computed from the integration of the momentum balances relative to the gas and the bubbly liquid phase:

$$(1-a_f)\frac{dp}{dX} = \frac{\tau_i S_i}{A} + \frac{\tau_{wb} P_b}{A} + \rho_G g(1-a_f)\sin\theta \quad [11]$$

and

$$\rho_L \frac{d}{dX}[(v_t - v_f)^2 a_f h_f] + a_f \frac{dp}{dX} + g\rho_L \cos\theta \frac{d}{dX}(a_f h_f \xi) = \frac{\tau_{wf} P_f}{A} - \frac{\tau_i S_i}{A} + a_f g \sin\theta[\rho_L h_f + \rho_G(1-h_f)]. \quad [12]$$

In [11] and [12] convective terms and the effect of the component of gravity normal to the flow direction relative to the gas phase have been neglected. The momentum exchange due to gas release from the film is also assumed negligible. In [11] and [12] p indicates pressure, P the wetted perimeter, S_i the interfacial chord, τ the shear stress, ρ the density, θ the pipe inclination, g the acceleration of gravity, ξ is the depth of the center of pressure, subscript i stands for interfacial and w for wall.

The wall stresses τ_{wb} and τ_{wf} can be evaluated as

$$\tau_{wb} = \tfrac{1}{2} f_b \rho_G v_b^2, \quad \tau_{wf} = {}^1\!f_{f\,L} v_f^2, \tag{13}$$

where the friction factors f_b and f_f are the same functions of the gas and liquid Reynolds numbers and of pipe roughness as in single-phase flow, with Re_{Gb} and Re_{Lf} defined as

$$Re_{Gb} = 4 \frac{A_b}{P_b + S_i} \frac{v_b}{\nu_G}, \quad Re_{Lf} = 4 \frac{A_f}{P_f} \frac{v_f}{\nu_L}. \tag{14}$$

In [14] ν indicates the kinematic viscosity. In the definition of τ_{wf}, the presence of dispersed bubbles is ignored, as it is assumed that these bubbles are only present in the bulk of the liquid and not in the wall region. The shear stress at the gas–liquid interface, τ_i, can be expressed as

$$\tau_i = \tfrac{1}{2} f_i \rho_G (v_b - v_f)^2, \tag{15}$$

where the interfacial friction factor, f_i, will be assumed as proportional to f_b:

$$f_i = B f_b. \tag{16}$$

The integration of [11] and [12] requires the use of continuity equations, [4] and [5], and of a mass balance relative to the gas dispersed in the liquid film. Assuming that the disengagement of gas bubbles is described by a turbulent transfer equation, this balance can be expressed as

$$A \frac{d}{dX} [(v_t - v_f) a_f (1 - h_f)] = -k_d S_i (1 - h_f). \tag{17}$$

In [17], k_d is, formally, a mass transfer coefficient. In this paper it is assumed that it scales as the rise velocity of a gas bubble in a stagnant liquid, v_d:

$$k_d = k v_d, \tag{18}$$

where the constant k can be derived from the experimental measurements of void in the slug tail. It is also assumed that, at least for air–water flow, the mean size of dispersed bubbles is such that their rise velocity is independent of size. In this case v_d is approximately given by

$$v_d = 1.18 \left(\frac{\sigma g (\rho_L - \rho_G)}{\rho_L^2} \right)^{0.25}, \tag{19}$$

where σ is the surface tension.

The initial conditions of [12] and [17] are

$$X = 0: a_f = 1, \quad h_f = h_s, \quad v_f = v_s. \tag{20}$$

These conditions are possibly verified at large mixture velocities, when the bubble nose is centered. According to Bendiksen (1984) this happens for values of the mixture Froude number, Fr_m, defined as

$$Fr_m = \frac{j_m}{\sqrt{gD}}, \tag{21}$$

where D is the pipe diameter, larger than 3.5. This flow configuration is obviously different from the stratified configuration on which [11] and [12] are based. Due to the gross approximations which lead to the formulation of these equations, their integration is only meaningful in the limiting case $Fr_m \to \infty$. In this case the influence of the component of the gravity vector normal to the flow direction becomes negligible also for the stratified liquid, and the term $g\rho_L \cos\theta [d(a_f h_f \xi)/dX]$ in [12] can be set equal to zero.

The model equations considered so far can easily be integrated for given values of h_s and l_s up

to the position $X = l_f$ at which the mass conservation equations, [1] and [2], are satisfied. Outputs of the model are the shape and void fraction of the slug tail, its final height, velocity and total length. For a given slug length, the slug frequency can easily be derived from the computed value of l_f as

$$v_s = \frac{v_t}{l_f + l_s}. \qquad [22]$$

The knowledge of the length of the slug unit allows the pressure gradient in slug flow to be computed from a momentum balance relative to the entire slug unit. As data relative to the pressure gradient are not considered in this work, the model is limited to the kinematic description of the flow structure.

4. RESULTS AND DISCUSSION

4.1. Slug flow characteristics

Typical time traces of slugs observed at a given location using the quarter ring probe and the pressure transducer are shown in figure 2. In these experiments two types of slugs have been observed:

- **Regular slugs,** in which it is possible to distinguish a *mixing zone* at the front, from a zone of approximately *constant void*, followed by the *bubble nose region*. An example of this type of slugs is shown in figure 2.
- **Shorter, more aerated slugs,** which have been classified by Nydal *et al.* (1992) as *developing slugs*. In these slugs it is not possible to detect the constant void region.

In relatively short pipes, these types of slugs are found over a wide range of gas and liquid flow rates and give rise to two distinct peaks in the probability distribution function of the mean void

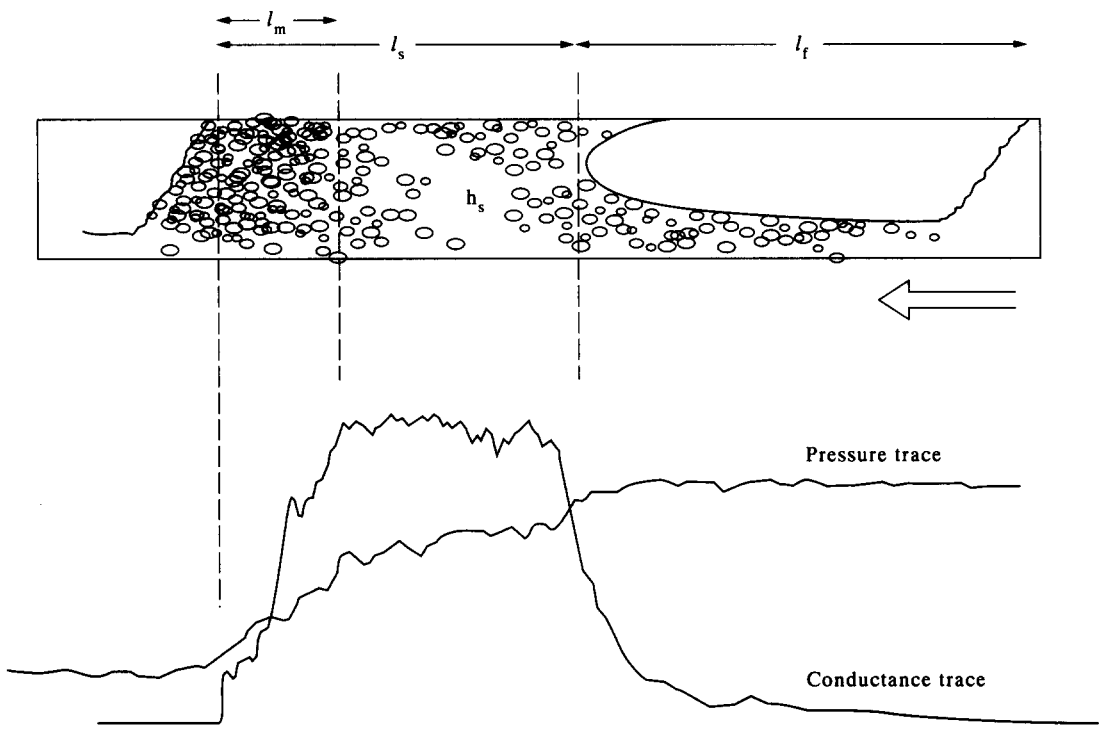

Figure 2. Schematic diagram of a slug unit with experimental time traces from an absolute pressure transducer and a conductance probe.

in the slugs (averaged void fraction in the constant void region for regular slugs, or peak void for developing slugs).

The experimental observations reported by Nydal *et al.* (1992) indicate that the two types of slugs travel at approximately the same translational velocity. This result and the analysis of the internal structure of developing slugs made with the optical probe indicates that developing or short slugs can easily be distinguished from waves or the so-called pseudo-slugs identified by Lin (1985).

Nydal *et al.* (1992) have given direct experimental evidence that developing slugs tend to grow to regular slugs in sufficiently long pipes. For this reason, in the present paper we focus our attention only on regular slugs, which are assumed to be typical of slug flow in long pipelines. The reported observation (Scott *et al.* 1987) that the slug length increases in long pipes should not modify the main experimental results reported in this paper.

The liquid holdup and pressure traces shown in figure 2 allow the identification of the three regions which characterize a liquid slug traveling in a pipe. Visual or high-speed camera observations confirm that the slug front is characterized by a chaotic, wavy region in which a stepwise increase in the liquid holdup is observed until the liquid front arrives to close the pipe cross section. The quarter ring probe starts to give a positive signal when the liquid front touches the upper wall. The mixing zone can then be considered to be the region of rapidly varying holdup or, as well, the region of steep increase in the pressure signal. In the constant void region the pressure signal increases with an approximately linear slope up to the bubble nose region, in which the pressure reaches an almost constant value.

Visual observations of the slug tail show that the bubble nose, in the range of mixture velocities analyzed in the present work, is centered. The liquid coming from the slug body is spread around the tip and for some distance it assumes an annular configuration before forming a stratified, aerated layer in the lower part of the pipe.

4.2. Slug length

The slug length (l_s in figure 2) can be computed from the transit time and the translational velocity of a slug at a measuring station. Transit times obtained from holdup signals depend on the discrimination level for the definition of a slug, because of the finite slopes in the holdup signal at the slug front and tail. With a level close to one half of the slug holdup, slug lengths determined from holdup measurements were in the range $l_s/D \approx 15$–22.

More precise values for l_s were obtained using two trigger probes spaced 8.5 diameters apart. The residence times corresponding to l_s and l_m (figure 2) were determined directly by visual observation at the computer screen of the time traces relative to single slugs using an interactive graphical software. The slug velocity was computed from the transit time which optimized the overlap of the time traces relative to the slug front arriving at the two probes. The mean values with standard deviations are shown in figure 3. As also observed by others (e.g. Nicholson *et al.* 1978), the slug length only weakly depends on the gas and liquid flow rates.

At low mixture velocities, when the entrainment of gas bubbles at the slug front is negligible, the slug length is approximately equal to $15D$; l_s then increases slightly to 17–D at large v_m. Nydal *et al.* (1992) reported values of l_s of the order of $18D$.

The length of the mixing zone in the front of the slug was obtained with the same procedure used for l_s. These results are also shown in figure 3. As can be seen, l_m can be fairly long: at large v_m it is almost one-half of the slug length. As in the experiments the mixing zone is associated with the presence of gas bubbles, it can only be detected when appreciable gas entrainment at the slug front occurs. The mixing zone can then be defined as the slug region characterized by a rapidly varying liquid holdup.

Dukler & Hubbard (1975) represented l_m as

$$l_m = \frac{0.15}{g}(v_m - v_f)^2. \qquad [23]$$

At large v_m, [23] largely overpredicts l_m. The present measurements are better correlated with the void fraction in the slug by the simple equation

$$\frac{l_m}{D} = k_m(1 - h_s) \qquad [24]$$

with $k_m \simeq 30$. This type of correlation can be justified on a qualitative basis, considering that both the length of mixing zone and the phenomenon of gas entrainment in the slug body are related to the formation of a steady vortex at slug front. Although the coefficient k_m is dimensionless, its value is possibly dependent on the physical properties of the gas–liquid mixture.

4.3. Aeration of the liquid film

The liquid from the slug may carry dispersed bubbles when entering the liquid layer under the slug bubble. Accurate measurements of the degree of aeration of the liquid layer are difficult, but some information on film aeration can be obtained with the local optical probe. The probe gives a binary output signal; high or low voltage, according to whether gas or liquid is detected at the probe tip. Local holdup fluctuations in slug flow are large and in order to obtain the mean holdup at a given position in the slug, ensemble averaging has been performed. A large number of time traces were recorded and superimposed (100–200 slugs). Examples of mean time traces from the trigger and the optical probe close to the bottom wall, are shown in figure 4. At the lowest gas flow rate the slug aeration close to the pipe wall is small, and the dispersed bubbles leave the film and enter the slug bubble after a short distance. At 7.5 mm from the wall the mean probe signal reaches a constant level in the slug bubble. At this position, the gas–liquid interface may occasionally be as low as the optical probe and contributes to a nonzero value of the void fraction in the film. This is also seen at the higher flow rates in the figure. At $j_G = 13.5$ m/s the film height can occasionally be < 5.0 mm. Table 1 reports the values, l_f, of the maximum distances from the bubble nose at which film aeration could be observed at 2.5 mm from the bottom wall.

These data can be used to estimate the value of the constant k in [18]. To this end, [11], [12] and [17] can be integrated for the given boundary conditions, [20], at varying values of k. It is found that for the limited set of data considered in table 1, the value $k = 0.26$ allows the void fraction in the slug tail to drop to 10% of the initial value at about the distances l_f from the bubble nose reported in table 1.

4.4. Local void distribution in the slug

The radial void distribution in the slug has been investigated with the local optical probe by superposition of time traces in a manner similar to the study of film aeration. Examples of mean

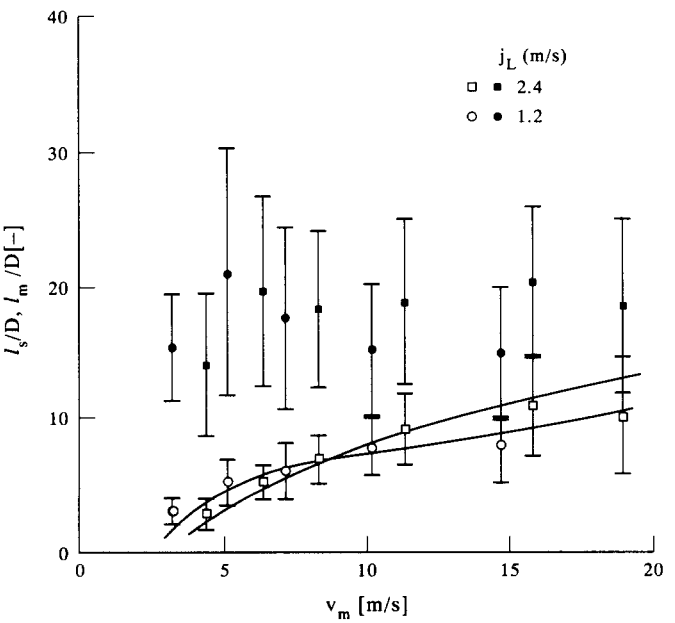

Figure 3. Length of slugs (l_s) and the highly aerated mixing zone in the slug front (l_m). The lines are predictions from [24] and the error bars are the standard deviations from the mean values (i.d. = 53 mm).

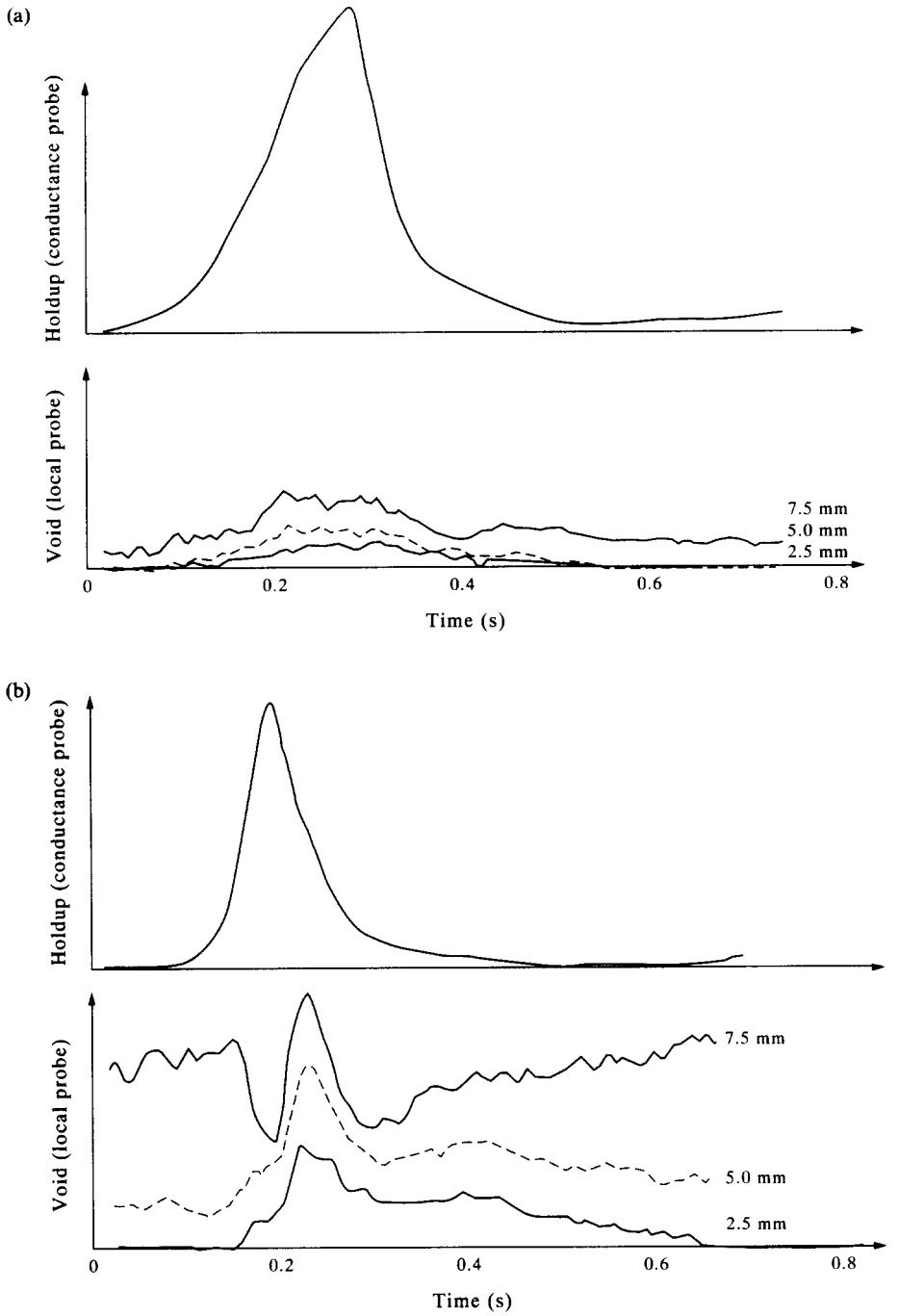

Figure 4. Superpositions of many time traces from the conductance probe and the local optical probe. The local probe was positioned 2.5, 5.0 and 7.5 mm from the bottom of the pipe (i.d. = 53 mm, $j_L = 1.2$ m/s). (a) $j_G = 6.0$ m/s; (b)$j_G = 13.5$ m/s.

Table 1. Length of the aerated zone of the liquid film under a slug bubble

j_L (m/s)	j_G (m/s)	l_f (m)
1.2	6.0	1.7
1.2	9.0	4.3
1.2	13.5	7.0

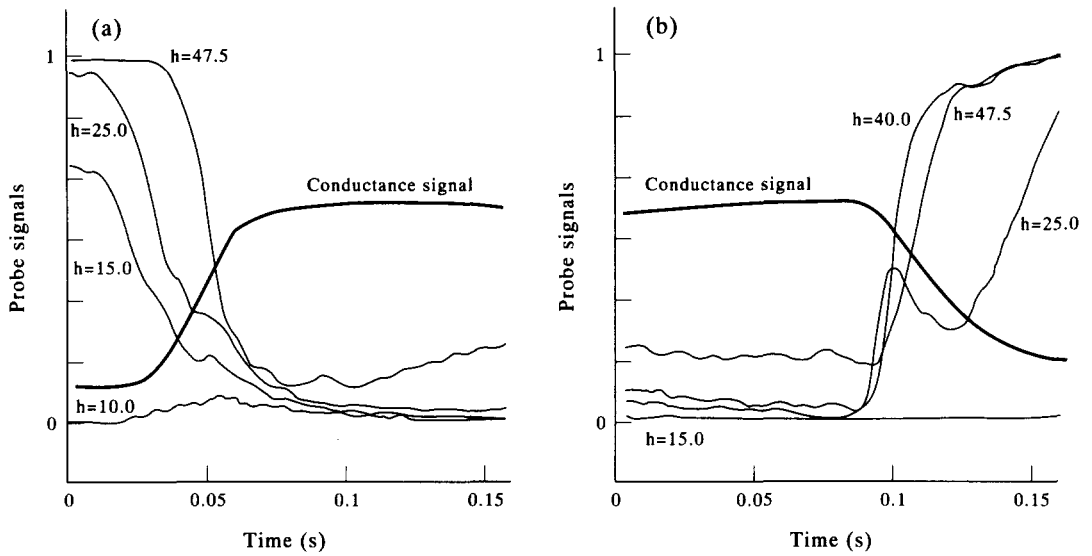

Figure 5. Example of results from the superposition of many slug traces from the conductance probe and the local probe. The position of the local pobe is relative to the bottom of the pipe (i.d. = 53 mm, $j_L = 1.2$ m/s and $j_G = 2.0$ m/s). (a) Slug front; (b) slug tail.

traces from the conductance probe and the optical probe at different positions in the cross section, are shown in in figure 5(a). In front of the slug, the high optical probe output corresponds to air, only, in the slug bubble. As the mean conductance trace is entered, the local fraction drops and reaches a near constant level, where the conductance signal levels out. This corresponds to the region immediately behind the highly aerated mixing zone, as illustrated in figure 2. Examples of time traces at the tail of the slug obtained in a similar manner, are shown in figure 5(b).

Mean values corresponding to the local void in the region behind the mixing zone at the slug front and the slug tail, are shown in figure 6 for various probe positions along the vertical diameter. At low flow rates the bubbles in the slug migrate to the upper wall as they propagate through the slug. At higher flow rates radial distributions tend to be symmetric both in the front and the tail of the slug. The aeration of the slug is then quite homogeneous.

To investigate the cross-sectional void distribution along the slug, a mean profile was computed from the superposition of many individual slug holdup profiles obtained from time traces. The results for several gas velocities are shown in figure 7. As can be seen, at intermediate flow rates there is, on an average, a void gradient along the slug. However, almost all data considered in this figure indicate that the void tends towards a constant value which is very close to the value determined by Nydal *et al.* (1992).

4.5. Size of dispersed bubbles in the slug

An estimate of the chordal size of the small bubbles in the slug was obtained from the local probe. The size of the bubbles was computed from the transit time of a bubble at the probe tip, assuming bubble velocities equal to the mixture velocity.

For each run, from 500 to 1000 bubbles were sampled from several slugs. An example of the statistical distribution of bubble chords is shown in figure 8. This is only an indication of the sizes, as accurate measurements should take into account the velocity of individual bubbles and a smaller probe tip than the actual one of 0.7 mm should be used. It may however be concluded that typical diameters of dispersed bubbles in air–water slugs are well below 5 mm.

4.6. Height of the stratified liquid layer

The presence of dispersed gas bubbles in the slug tail does not allow a simple analysis of the conductance signal obtained from the ring probe. For this reason, in this paper only measurments relative to the film height immediately ahead of an advancing slug are considered as, in this case, film aeration can be assumed to be negligible, at least for air–water flow at low liquid rates.

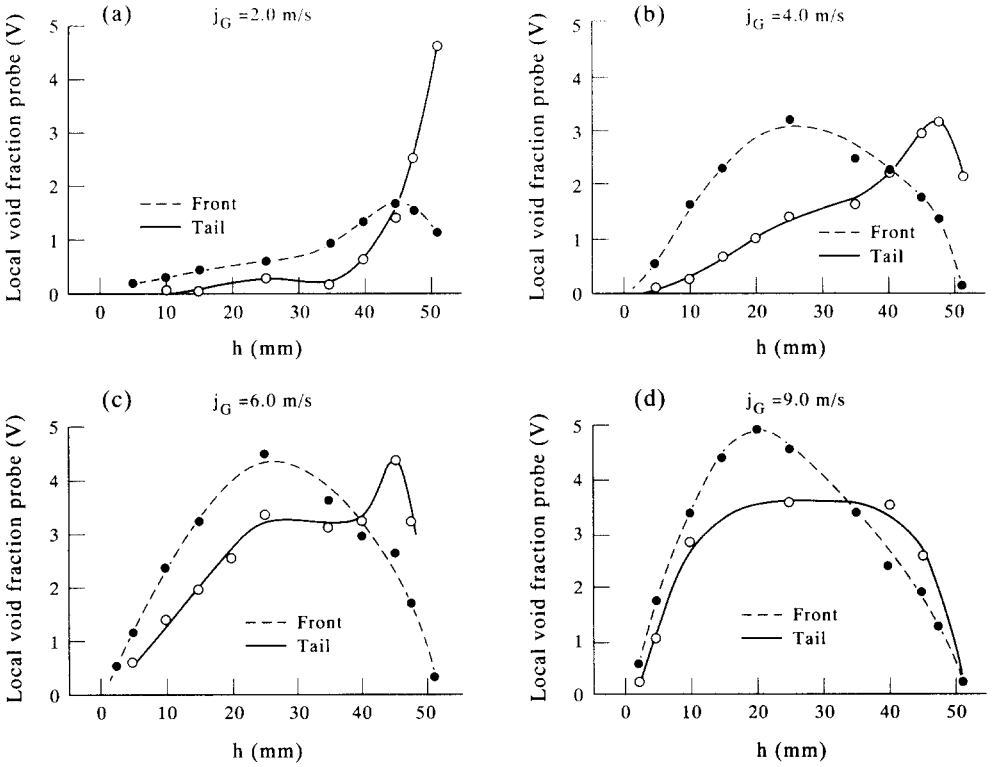

Figure 6. Mean radial void profile at the front (– – –) and at the tail (——) of the slugs ($j_L = 1.2$ m/s, i.d. = 53 mm).

Experimental measurements relative to the height of the liquid layer before an advancing slug are compared with theoretical predictions in figure 9. The predicted values of film height have been computed with the model outlined in section 3, assuming that the slug length is equal to 15*D* in all cases. This choice is related to the presence of an aerated mixing zone in front of a slug. In this zone the liquid holdup is appreciably less than in the constant void region. The overall effect of the mixing zone can then be assumed to be an appreciable reduction in the value of slug length used to predict main slug parameters. In this work, we assume that the actual slug length is, in all cases, equal to the length found in the absence of gas entrainment, i.e. about 15*D*. This value

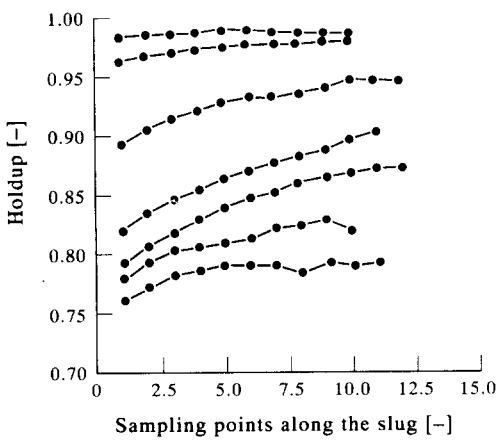

Figure 7. Mean cross-sectional holdup profiles along the slugs from the superposition of many time traces (v_m = 1.2, 2.5, 3.6, 4.5, 5.4, 6.4 and 7.7 m/s, i.e. = 31 mm).

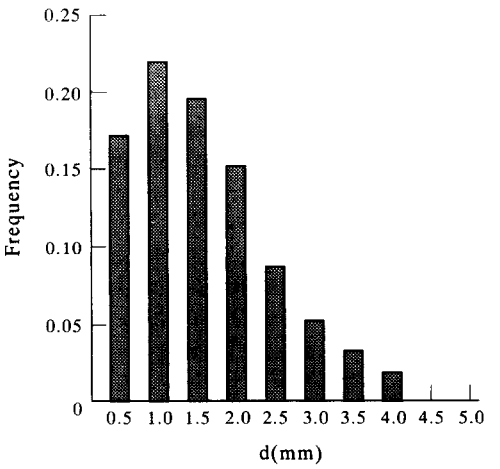

Figure 8. Statistical distribution of the cordial size of dispersed bubbles in the slugs (j_L = 1.2 m/s, j_G = 2.0 m/s, i.d. = 53 mm).

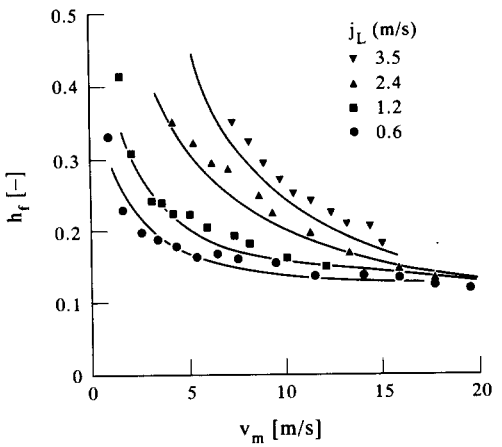

Figure 9. Experimental and computed holdup in the film region in front of the slugs.

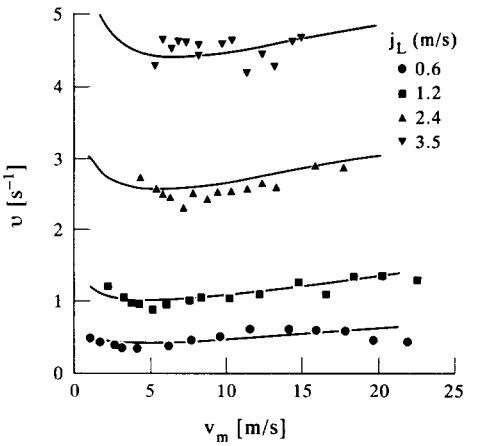

Figure 10. Experimental and computed slug frequencies (i.d. = 53 mm).

is considerably smaller than the value of $30D$ found by Nicholson *et al.* (1978) and used by them to close their model. This difference is probably related to the different geometry (inlet section, pipe length) and different method used by these authors to evaluate l_s.

In any case, the final height of the stratified liquid layer is only a weak function of the assumed value of l_s. Therefore, the good agreement between the theory and experiments found in figure 9 should not be attributed to the choice made for l_s.

4.7. Slug frequency

The slug frequency is related to the length of the slug unit by [22]. In the present work it has been decided to measure v_s rather than l_u of l_f, as this measurement is simpler from a practical standpoint: once a threshold value for the liquid holdup in a slug is established, the frequency can be obtained from the number of slugs counted in a given time interval. The threshold value has been fixed on the basis of the extensive statistical analysis of slug flow reported by Nydal *et al.* (1992).

In all the experiments performed, there were very limited uncertainties about the classification as slugs (regular or developing slugs) of the observed phenomena, mainly because no experiments at low liquid flow rates, close to the transition to stratified flow, have been performed. As a matter of fact, close to this transition the slug frequency is too closely related to the geometry of the pipe (inlet configuration, pipe length) to allow a reliable measurement of slug frequency, while at higher liquid flows the present observations only indicate a weak dependence of slug frequency or length on the pipe geometry.

Measured values of frequency are compared with computed values in figure 10. As can be seen, the agreement is excellent thus indicating that the flow model presented in this paper is able to give a good representation of the flow structure.

5. CONCLUSIONS

A charcterization of the holdup distribution in horizontal, air–water slug flow in pipes of 50 and 90 mm i.d. has been made from local and cross-sectional void fraction measurements. The main experimental results are the following:

- Measured slug lengths are quite independent of flow rates, and the values are in the range reported by other authors. The length of the highly aerated mixing zone in the front of the slugs is large and can extend up to one-half of the slug length at high velocities.
- At intermediate velocities there is a void gradient along the slug, whereas at high velocities the aeration in the front and the tail of the slug is fairly constant.
- The diameters of small dispersed bubbles in a slug are well below 5 mm.

- Measurements with the local optical probe indicate that the aeration of the liquid layer under the slug bubble can extend significantly into the slug bubble region.

On the basis of the present experimental observations, an improved $1/D$ model of slug flow is proposed. The model gives very good predictions of the height of the stratified liquid layer at the slug front and of the slug frequency.

Acknowledgements—O. J. Nydal acknowledges the fellowship received by the Norwegian Council for Technical Research (NTNF). This work has been partially supported by the Commission of the European Communities, under Contract EN3G-0037/I.

REFERENCES

ANDREUSSI, P., DI DONFRANCESCO, A. & MESSIA, M. 1988 An impedance method for the measurement of liquid hold-up in two-phase flow. *Int. J. Multiphase Flow* **6,** 777–787.

ANDREUSSI, P., MINERVINI, A. & PAGLIANTI, A. 1993 A mechanistic model of slug flow in near-horizontal pipes. *AIChE Jl.* In press.

ANNUNZIATO, M. 1986 Catena di misura con sonde a fibra ottica per il rilievo della frazione di vuoto. Report NQDM 1TS4B 86039.

BENDIKSEN, K. H. 1984 An experimental investigation of the motion of the long bubbles in inclined tubes. *Int. J. Multiphase Flow* **6,** 797–812.

DUKLER, A. E. & HUBBARD, M. G. 1975 A model for gas–liquid slug flow in horizontal and near horizontal tubes. *Ind. Engng Chem. Fundam.* **14,** 337–347.

LIN, P. Y. 1985 Flow regime transitions in horizontal gas–liquid flow. Ph.D. Thesis, Univ. of Illinois, Urbana, IL.

NICHOLSON, M. K., AZIZ, K. & GREGORY, G. A. 1978 Intermittent two phase flow in horizontal pipes: predictive models. *Can. J. Chem. Engng* **56,** 653–663.

NYDAL, O. J., PINTUS, S. & ANDREUSSI, P. 1992 Statistical characterization of slug flow in horizontal pipes. *Int. J. Multiphase Flow* **18,** 439–453.

SCOTT, S. L., SHOHAM, O. & BRILL, J. 1987 Modelling slug growth in large diameter pipes. Presented at the *3rd Int. Conf. on Multi-phase Flow*, The Hague, Netherlands.